Research and design a model of 2D profile generation system applied in laser welding technology using piezo linear actuators

Nguyen Trong Khuyen[1], Tran Quang Phuoc[2*]

[1]Control, Automation in Production and Improvement of Technology Institute (CAPITI), Vietnam;
[2]Faculty of Mechanical Engineering, Ho Chi Minh City University of Technology (HCMUT), Vietnam.
[*]Corresponding author: tqphuoc@hcmut.edu.vn

Received 6 Nov. 2023; Revised 28 Dec. 2023; Accepted 6 Feb. 2024; Published 25 Feb. 2024.
DOI: https://doi.org/10.54939/1859-1043.j.mst.93.2024.137-145

ABSTRACT

The article introduces a method to create any 2D laser profiles applied in welding technology. This method allows for the creation of profiles that best suit the weld characteristics and material of the weld workpiece, thereby improving the quality, accuracy, and aesthetics of the weld and increasing laser welding efficiency. In the study, the authors proposed a model of a 2D laser profile generation system with a reflecting mirror and two piezoelectric linear actuators. The forward and inverse kinematic equations were completely solved, while a control algorithm was proposed to control the motion of linear actuators. The model is simulated on MATLAB with circular, sin-wave, and 8-figured profiles. The obtained results show that the control profiles are almost close to the desired ones (both shape and scan period). There is a displacement between them. With the given simulation parameters, the displacements of the above-mentioned profiles are 0.03 mm (1.5%), 0.05 mm (2.5%), and 0.05 mm (1.25%), respectively. This shifting can be reduced by increasing the number of samplings. The simulation results provide strong evidence for the feasibility of implementing a practical 2D laser profile generation system based on the proposed model.

Từ khóa: Laser profile; Laser welding; Non-contact welding; Piezo linear actuator.

1. INTRODUCTION

The laser was first introduced in 1960 by Theodore Maiman at Hughes Laboratory [1]. Laser beams can be focused on very tiny spots with high irradiance. Over a period of decades, laser technology has been constantly developed and has made big achievements in a wide range of high-technology fields (optical art projection, military, laser welding, biological technology, etc.).

Despite being more costly, laser welding has witnessed an increasing adoption due to its advantages over traditional methods [2, 3]. Due to the fact that laser radiation can be constrained in a very narrow beam and not scatter when going far away from its source, it allows to control laser energy focusing on a small area with high density. By directly heating with a laser beam, the temperature of local regions of workpieces can increase quickly, while other zones of the material remain cold. As a result, different parts and even different metals are joined in a non-contact process. This minimizes heat loss and time consumption, increases productivity, and allows the implementation of regular, aesthetically pleasing welds in restricted conditions with minimal intervention. Laser welding technology continues to be optimized with research into spatter formation, which gives insights into the welding process and increases the effectiveness of welding practices [4]. Research also focused on beam oscillation patterns, which estimate their effect on weld characterization [5]. Studies then concentrated on laser welding for different types of materials, for example, plastics, alloys, dissimilar metals, or the optimization of methodologies for the laser welding process [6–8].

Basically, laser welding attaches to the procedures of creating laser profiles and then translating and overlapping them. The laser source must not be focused for too long at one point and must be projected evenly within the profile during the welding process. To increase efficiency, profiles need to be generated with a shape and dimension that best suit the weld's characteristics and

materials of welding workpieces. In the laser welding industry, profile creation can be performed using single-axis or two-axis mechanisms. The structure using a single shaft is relatively popular because this method is easy to manufacture and control and can be used in cases of low requirements. The drawback of this structure is that it only creates basic profiles of circular shapes. The 2-axis profile scanning mechanism has a more complex structure, using two sets of galvanometer mirrors. It allows the creation of profiles of any figure, but the scanning speed is limited by the maximal oscillation frequency of the galvanometers, and the structure is relatively bulky. Its profile ranges are dependent on the dimensions of the mirrors and the distance between them. These disadvantages can be overcome with a proposed model using a reflecting mirror and piezo linear actuators. The new advanced approach permits the generation of any 2D profile while reducing the dimension of the mirror to a minimum. The reduction in the dimension of the reflecting mirror does not affect profile ranges as long as a laser beam falls into the mirror area; hence, it totally reduces the dimension of the structure.

In this article, the authors present research and the design of a 2D profile generation system. Piezo linear actuators, which have small dimensions and high precision in displacement control (nanoscale), are proposed to be used [9]. In the framework of the research, a system model is introduced. The forward and inverse kinematics equations are fully resolved, while an advanced algorithm is proposed and simulated.

2. METHODOLOGY

2.1. The model of 2D profile generation system

A laser application consists of different parts, basically, it includes a laser source, laser fiber optic, profile generation system, focus lens, and profile screen (Fig. 1).

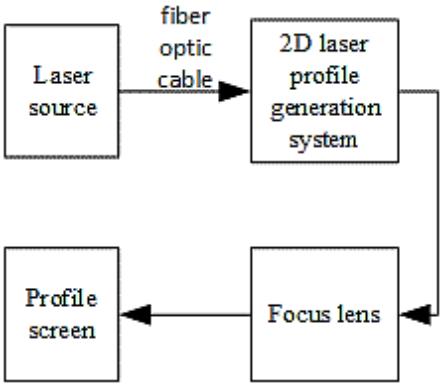

Figure 1. *The basic block diagram of a laser application.*

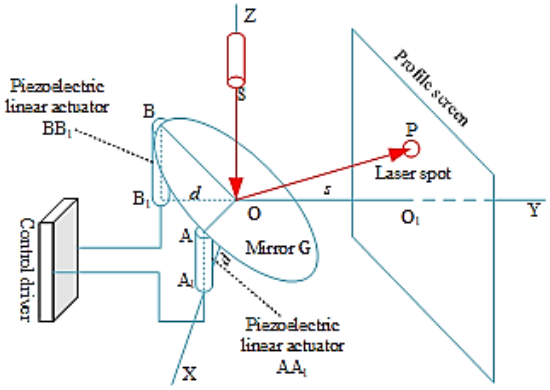

Figure 2. *Proposed 2D laser profile generation system.*

In the framework of the paper, we only focus on the 2D laser profile generation system. The system is constructed from one reflecting mirror, two piezo linear actuators, and a control driver. Laser beams reflect only on one mirror before going to the profile screen. This, on some scale, can reduce the loss of the laser beam in comparison to the case of a two-axis profile scanning system. In the model, the mirror has a rigid center O. Two piezo linear actuators, AA1 and BB1 are located at a distance of d from the center. They change their displacement in the OZ direction. As a result, the mirror rotates around the center. In order to get the desired profile, an advanced algorithm is introduced to control these two piezo linear actuators. For building kinematic equations, we choose a coordinate system OXYZ with the origin at the center O. The laser source is arranged on the OZ axis, emitting a laser beam to the center of the mirror, while the AA_1 and BB_1 actuators are arranged in the OXZ and OYZ planes, respectively. The profile screen is perpendicular to the OY axis and keeps a distance of s from the coordinate origin. Some parameters of the model are listed in table 1.

Table 1. *Parameters of the model.*

Parameters	Units	Description	Parameters	Units	Description
Mirror G:			*Laser source S:*		
Radius, R_G	mm	The radius of the mirror	Cross section, S_{cross}	mm^2	Cross section of laser beam
Piezo linear actuator AA_1:			*Piezo linear actuator BB_1:*		
Travel range, X_A	mm	The travel range of the actuator AA_1	Travel range, X_B	mm	The travel range of the actuator BB_1
Resolution, S_A	nm	The minimum travel of the actuator AA_1	Resolution, S_B	nm	The minimum travel of the actuator BB_1
Profile:			*Position arrangement:*		
Y- Range, R_Y	mm	Dimension of profile in Y-direction	Distance, d_{sp}	mm	The distance from the profile-screen to the coordinate origin, default *s*
Z- Range, R_Z	mm	Dimension of profile in Z-direction	Distance, d_{AA1}	mm	The distance from actuator AA_1 to the origin O, default *d*
Scanning period, T_{scan}	ms	Profile scanning period	Distance, d_{BB1}	mm	The distance from actuator BB_1 to the origin O, default *d*
Piezo control driver:					
Input co mmand		Control co mmand to driver	Output range,V_O	V	The output voltage applying to piezoelectric actuator

2.2. Piezo linear actuator

Piezo linear actuators are based on a special characteristic of materials that produce displacement and force when electrical energy is applied to them. The advantages of piezoelectric linear actuators over other types are higher displacement accuracy, a larger generation force, and a higher response speed. Furthermore, it consumes low energy, has no heat generation, and has no moving parts like gears or bearings. For the model, we can use closed-loop piezo linear actuators with a travel range of ~1 mm, precision of < 30 nm, and a frequency of 5 kHz. This kind of device has a travel range that meets the travel range required in simulation on Matlab (the travel range of linear actuators in the simulation was smaller than 1 mm).

Figure 3. *Example of the piezo linear actuator and its driver.*

2.3. The forward kinematic equation

Based on the proposed model, we have the coordinates of the points A = (*d, 0, Z_A*), B = (*0, -d, Z_B*), $Z_B > 0$. Let $e_1 = (1, 0, 0)$, $e_2 = (0, 1, 0)$, $e_3 = (0, 0, 1)$ – unit vectors of the OX, OY and OZ axes, $\vec{n}$ - the normal of the mirror. We have:

$$\vec{n} = k\left[\overrightarrow{OB}, \overrightarrow{OA}\right] = k\begin{bmatrix} e_1 & e_2 & e_3 \\ 0 & -d & Z_B \\ d & 0 & Z_A \end{bmatrix} = k\left(-dZ_A, dZ_B, d^2\right) = dk\left(-Z_A, Z_B, d\right) \quad (1)$$

While *k* is a scale value. Let *k* be chosen to ensure *dk = 1*. Then (1) can be rewritten as:

$$\vec{n} = \left(-Z_A, Z_B, d\right) \quad (2)$$

Let $\vec{p}$ - The normal of the laser beam from the source S, $\vec{p} = -\vec{e}_3 = (0,0,-1)$. Let $\vec{q} = -\vec{p} = (0,0,1)$ and $\vec{q}_{\|\vec{n}}$ - The projection of the vector $\vec{q}$ on the vector $\vec{n}$. We have:

$$\vec{\mathrm{q}}_{\|\vec{n}} = \cos(\angle(\vec{q},\vec{n}))|\vec{q}|\frac{\vec{n}}{|\vec{n}|} = \frac{(\vec{q},\vec{n})}{|\vec{q}||\vec{n}|}|\vec{q}|\frac{\vec{n}}{|\vec{n}|} = \frac{(\vec{q},\vec{n})}{|\vec{n}|^2}\vec{n} = \frac{d\left(-Z_A, Z_B, d\right)}{Z_A^2 + Z_B^2 + d^2} = \frac{(-\alpha,\beta,1)}{\alpha^2+\beta^2+1} \quad (3)$$

Where $\alpha = Z_A / d$, $\beta = Z_B / d$. Let $\vec{m}$ - The normal of the reflecting laser beam on the mirror. Based on the nature of reflection on a flat mirror, we have:

$$\vec{m} + \vec{q} = 2\vec{q}_{//\vec{n}} \quad (4)$$

$$\Rightarrow \vec{m} = 2\vec{q}_{//\vec{n}} - \vec{q} = \frac{2(-\alpha,\beta,1)}{\alpha^2+\beta^2+1} - (0,0,1) = \frac{\left(-2\alpha, 2\beta, 1-\alpha^2-\beta^2\right)}{\alpha^2+\beta^2+1} \quad (5)$$

Let P – Laser spot on the profile screen. P is the intersection of the profile screen (described by *Y = s*), and the laser-reflecting beam (described by $\vec{r} = \vec{m}t$). Resolve the system functions:

$$\vec{r} = \vec{m}t;\ Y = s \quad (6)$$

We have the coordinates of laser spot P:

$$X = \frac{-s\alpha}{\beta} = \frac{-sZ_A}{Z_B} \quad (7)$$

$$Y = s \quad (8)$$

$$Z = \frac{s(1-\alpha^2-\beta^2)}{2\beta} = \frac{s(d^2 - Z_A{}^2 - Z_B{}^2)}{2dZ_B} \quad (9)$$

The formulas (7), (9) describe the forward kinematic equation for the scanning model. For X-coordinate, when $Z_A \to 0$, $X \to 0$, while $Z_B \to 0, X \to \infty$. For *Z*-coordinate, when $Z_A{}^2 + Z_B{}^2 \to d^2$, $Z \to 0$, while $Z_B \to 0$, $Z \to \infty$. So, by changing the values of Z_A, Z_B, we can expand the profile at any scale in two directions: OX and OZ.

2.4. The inverted kinematic equation

In this problem, we have a profile on a plane described by a parameter function. The aim of the research is to propose a control method to derive the desired profile. It is clear that any curve in the 2D plane can be approximated by a set of parameter functions, for example, cubic spline interpolation. Let's take a look at a profile described by a set $\hat{P}$ = { $\hat{P}_1$, $\hat{P}_2$, …, $\hat{P}_n$ }, where $\hat{P}_i$ - A parameter function denotes piece number *i*. $\hat{P}_i$ can describe as:

$$\hat{P}_i(t) = \begin{bmatrix} X_i(t) \\ Z_i(t) \end{bmatrix},\ t \subset [t_i, t_{i+1}] \quad (10)$$

where t_i is the breaking point of parameter *t*. The length of $\hat{P}_i$ is determined by the formula:

$$l_i = \int_{t_i}^{t_{i+1}} \sqrt{\dot{X}_i^{\,2}(t) + \dot{Z}_i^{\,2}(t)}\,dt \tag{11}$$

Let v_i - Speed of laser spot motion when moving on the piece $\widehat{P}_i$; T_i - The time for laser spot traveling along the piece $\widehat{P}_i$. In the case of regular motion on $\widehat{P}_i$. We have:

$$v_i = l_i / T_i \tag{12}$$

If the speed of the laser spot remains unchanged on the total profile $\widehat{P}$, so we have:

$$v = l / T = \sum_{i=1}^{n} l_i / \sum_{i=1}^{n} T_i = v_i = l_i / T_i \tag{13}$$

Where $l = \sum_{i=1}^{n} l_i$ - The length of the total profile, while $T = \sum_{i=1}^{n} T_i = T_{scan}$ - The total scanning time.

Let t_{real} – Real-time parameter, $t = t(t_{real})$. The instantaneous speed of a laser spot is defined as:

$$v(t_{real}) = v_i(t_{real}) = \frac{dl_i}{dt_{real}} = \frac{\sqrt{\dot{X}_i^{\,2}(t) + \dot{Z}_i^{\,2}(t)}\,dt}{dt_{real}} = \frac{l_i}{T_i} \Rightarrow \frac{dt}{dt_{real}} = \frac{l_i}{T_i\sqrt{\dot{X}_i^{\,2}(t) + \dot{Z}_i^{\,2}(t)}} \tag{14}$$

Take the derivative of the left part of (7) with respect to t_{real}, we have:

$$\frac{dX}{dt_{real}} = \frac{dX_i}{dt}\frac{dt}{dt_{real}} = \frac{\dot{X}_i l_i}{T_i\sqrt{\dot{X}_i^{\,2} + \dot{Z}_i^{\,2}}} \tag{15}$$

On the other hand, take the derivative of the right part of formula (7):

$$\frac{d}{dt_{real}}\left(\frac{-sZ_A}{Z_B}\right) = \frac{s(-\dot{Z}_A Z_B + Z_A \dot{Z}_B)}{Z_B^2} \tag{16}$$

From (16) and (17), we have:

$$\frac{l_i \dot{X}_i}{T_i\sqrt{\dot{X}_i^{\,2} + \dot{Z}_i^{2}}} = -\frac{s}{Z_B}\dot{Z}_A + \frac{sZ_A}{Z_B^2}\dot{Z}_B \tag{17}$$

Similarly, if we take the derivative of (8) with respect to real-time t_{real}, we get:

$$\frac{l_i \dot{Z}_i}{T_i\sqrt{\dot{X}_i^{\,2} + \dot{Z}_i^{2}}} = \frac{-sZ_A}{dZ_B}\dot{Z}_A + \frac{s(Z_A^{\,2} - Z_B^{\,2} - d^2)}{2dZ_B^{\,2}}\dot{Z}_B \tag{18}$$

In the case when the speed of the laser spot remains unchanged at l / T_{scan}, we have:

$$\frac{l\dot{X}_i}{T_{scan}\sqrt{\dot{X}_i^{\,2} + \dot{Z}_i^{2}}} = -\frac{s}{Z_B}\dot{Z}_A + \frac{sZ_A}{Z_B^2}\dot{Z}_B;\quad \frac{l\dot{Z}_i}{T_{scan}\sqrt{\dot{X}_i^{\,2} + \dot{Z}_i^{2}}} = \frac{-sZ_A}{dZ_B}\dot{Z}_A + \frac{s(Z_A^{\,2} - Z_B^{\,2} - d^2)}{2dZ_B^{\,2}}\dot{Z}_B \tag{19}$$

By using a recursive process, we can calculate the dynamic parameters of the model in real time.

2.5. Control algorithm

A proposed control algorithm is shown as a follow-up chart in Fig. 4. Two linear actuators AA_1 and BB_1 are controlled to change their displacements, then change the direction of the laser beam in X- and Z-directions. The initial values of parameters Z_A, Z_B are inferred from (7), (9):

$$Z_{A-init} = \frac{dX_0\left(Z_0 - \sqrt{s^2 + X_0^2 + Z_0^2}\right)}{(s^2 + X_0^2)};\quad Z_{B-init} = \frac{ds\left(-Z_0 + \sqrt{s^2 + X_0^2 + Z_0^2}\right)}{(s^2 + X_0^2)} \tag{20}$$

Where N – Number of samplings. In the recursive process, we take the discreteness of these control parameters. The value of dt is calculated using the following formula (14), while V_A, V_B - Derivatives of Z_A, and Z_B are inferred from (19). The values of Z_A and Z_B are calculated by the discrete integration of V_A, V_B. These values are then converted to control co mmands and passed to the piezo linear actuator control driver. The loop will end when the number of iterations reaches the predetermined sampling number N.

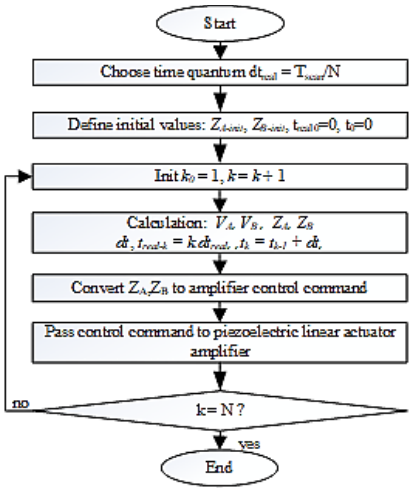

Figure 4. *The flow char of the control algorithm for one scan.*

3. SIMULATION AND RESULTS

For a circular profile, the input parameters are described in table 2. Fig. 5 shows the displacements of linear actuators AA_1 and BB_1 over real-time, while Fig. 5 compares the obtained circular profile with the profile defined by the parameter function. Displacement of control figure: 0.03 mm/2 mm (1.5%).

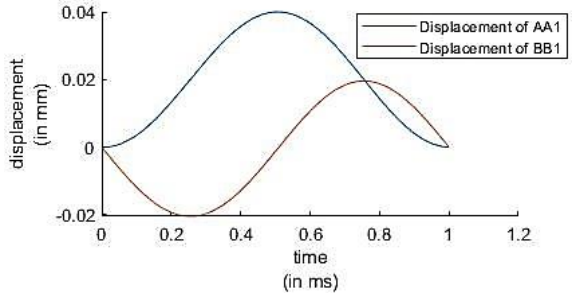

Figure 5. *The displacements of linear actuators over real-time for the circular profile.*

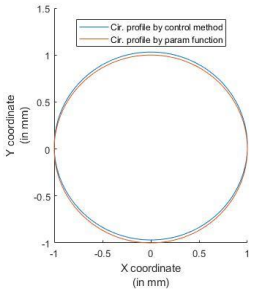

Figure 6. *Circular profiles are obtained by the control method and by parameter function.*

Table 2. *Parameters of a circular profile.*

Parameter	T_{scan} = 1 ms	N = 100	dt_{real} = 0.01 ms	s = 100 mm	d = 2 mm
Profile	Parameter function			Shape	
Circular	$\begin{cases} X = \cos(t) \\ Z = \sin(t) \end{cases}, \ t \in [0, 2\pi]$				

For a sine-wave profile, input parameters are described in table 4. The initial coordinates of points A and B are defined by the formula (22), $Z_{A\text{-init}}$ = 0 (mm), $Z_{B\text{-init}}$ = 2 (mm). Fig. 7 shows the displacements of linear actuators AA_1 and BB_1 over real-time, while Fig. 8 compares the obtained circular profile and the profile defined by the parameter function. Displacement of control figure: 0.05 mm/2 mm (2.5%).

Table 3. *Simulation results for the circular profile.*

t_{real} (ms)	t	V_A (mm/ms)	V_B (mm/ms)	*Displacement Of* AA_1 (mm)	*Displacement Of* BB_1 (mm)	*Controlled profile*	
						X(mm*)*	*Y(* mm*)*
0	0	0.0013	-0.1257	0	0	1.0000	1.0000
0.01	0.0628	0.0091	-0.1252	0.00001	-0.00125	0.9960	0.9960
0.02	0.1257	0.0170	-0.1243	0.00010	-0.00250	0.9881	0.9881
……	……	……	……	……	……	……	……
1	6.2832	0.0013	-0.1257	0.00000	0.00000	1.0000	0.00000

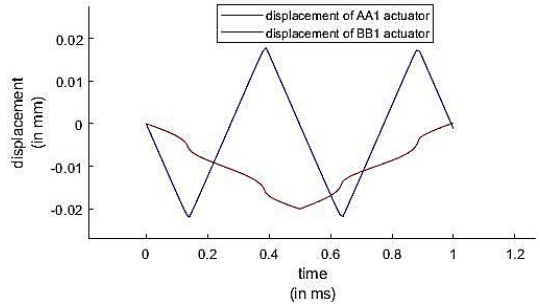

Figure 7. *The displacements of linear actuators over real time for sine-wave profile.*

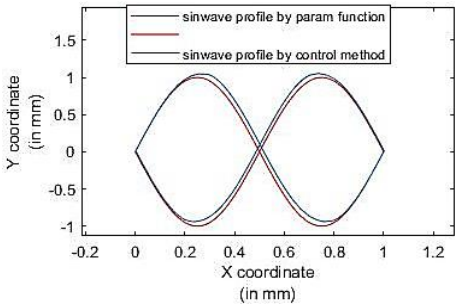

Figure 8. *Sin-wave profiles obtained by control method and by parameter function.*

Table 4*. Parameters for a sine-wave profile.*

Parameter	T_{scan} = 1 ms	N = 100	dt_{real} = 0.01 ms	s = 100 mm	d = 2 mm
Profile	Parameter function			Shape	
Sin-wave	$\begin{cases} P_1(t) = \begin{cases} X = t \\ Z = \sin(2\pi t) \end{cases}, & t \in [0,1]; \\ P_2(t) = \begin{cases} X = -t + 2, \\ Z = \sin(2\pi t) \end{cases}, & t \in [1,2] \end{cases}$				

For any profile with spline interpolation description, for instance, the 8-figured profile depicted by cubic spline interpolation, input parameters are shown in table 5. Table 6 shows simulation results for the 8-figured profile. Fig. 9 depicts the displacement of linear actuators over time for an 8-figured profile, while Fig. 10 compares the obtained 8-figured profile and the profile defined by the parameter function. They almost coincide. Displacement of control figure: 0.05 mm/4 mm (1.25%). Fig. 10 shows the obtained profiles with different values of sampling number *N*.

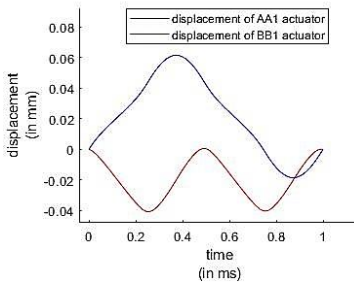

Figure 9. *The length of linear actuators over real-time for 8-figured profile.*

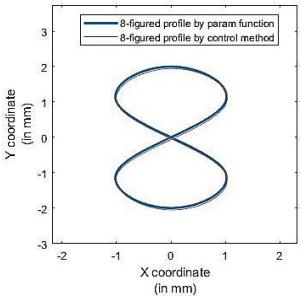

Figure 10. *8-figured profiles by proposed method and by parameter function.*

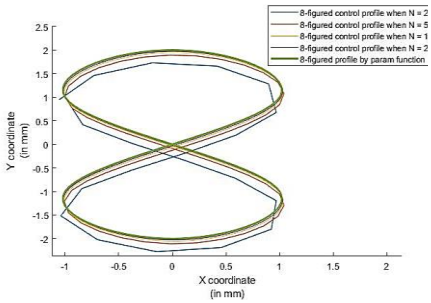

Figure 11. *8-figured profiles with N = 10, 50, 100, 200.*

Simulation results show that by applying the proposed method, we derive control profiles that are almost close to the desired figures and reach the desired scanning period. This shows the rightness of the theoretical results in the paper. There is a displacement between these two profiles. By decreasing time sampling, we can minimize this shifting, but it will increase the volume of calculations.

Table 5. *Parameters for an 8-figured profile.*

Parameter	T_{scan} = 1 ms	N = 100	dt_{real} = 0.01 ms	s = 100 mm	d = 2 mm
Profile	Parameter function (Cubic spline interpolation)				Shape
8-figured	Breaks: [0 1.6818 2.8710 4.0602 5.7420 6.9312 8.1204]; pieces: 6, order: 4, dim: 2; coefs: [12×4 double]: -0.5946 1.5000 0.3483 -1.0000 -0.5946 1.5000 0.3483 -1.0000 -0.0248 0.0624 -1.2242 1.0000 0.0248 -0.0624 1.2242 -1.0000 0.4204 -1.5000 0.3483 1.0000 0.4204 -1.5000 0.3483 1.0000 0.3236 -0.0624 -1.2242 -1.0000 -0.3236 0.0624 1.2242 1.0000 0.4204 -0.0000 -1.4355 0 0.4204 -0.0000 -1.4355 0 -0.3236 1.0919 0.0000 -2.0000 0.3236 -1.0919 0 2.0000				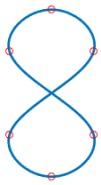

Table 6. *Simulation results for the 8-figured profile.*

t_{real} (ms)	t	V_A (mm/ms)	V_B (mm/ms)	*Displacement of* AA_1 (mm)	*Displacement of* BB_1 (mm)	*Controlled profile*	
						X (mm)	Y (mm)
0	0	-0.0636	0.2324	0	0	-1.0000	1.0000
0.01	0.0956	-0.1076	0.2159	-0.0006	0.0023	-0.9667	0.8830
0.02	0.1850	-0.1367	0.1991	-0.0017	0.0045	-0.9115	0.7746
0.03	0.2678	-0.1557	0.1850	-0.0031	0.0065	-0.8418	0.6750
……	……	……	……	……	……	……	……
0.98	7.9231	0.0405	0.2370	-0.0003	-0.0047	-0.9885	1.2402
0.99	8.0223	-0.0105	0.2404	0.0001	-0.0024	-1.0078	1.1201
1	8.1214	-0.0641	0.2323	0.0000	0.0000	-1.0012	0.9987

4. CONCLUSIONS

To conclude, the paper successfully introduces a practicable methodology to build advanced 2D profile generation systems in laser welding technology, enabling the enhancement of the quality, precision, and adaptability of welding techniques. The research has been carefully simulated through Matlab with circular, sin-wave, and 8-figured profiles and has obtained laser profiles closely approximating the desired figures with displacements of 0.03 mm (1.5%), 0.05 mm (2.5%), and 0.05 mm (1.25%), respectively. These simulation results provide strong evidence of the feasibility of implementing the proposed model to build a real-profile generation system for laser applications. In further research, the paper can focus on enhancing and fine-tuning the control algorithm and optimizing the structure of the system to minimize divergence between the obtained and desired profiles.

REFERENCES

[1]. Kenichi Iga, "*Fundamentals of Laser Optics*", Springer, (1994).
[2]. Nasir Ahmed, "*New developments in advanced welding*", Woodhead publishing (2005).
[3]. M. T. Andani, et al., *"Spatter formation in selective laser melting process using multi-laser technology",* Materials and Design, Vol. 131, pp. 460-469, (2017).
[4]. Lei wang, et al., *"Effect of beam oscillating pattern on weld characterization of laser welding of AA6061-T6 aluminum alloy",* Materials and Design, Vol. 138, pp. 707-717, (2016).
[5]. Rolf Klein, *"Laser welding of plastics",* Wiley-VCH, (2012).
[6]. Pengfei Wang, *et al.*, "*Laser welding dissimilar materials of aluminum to steel: an overview*", The International Journal of Advanced Manufacturing Technology, pp. 3081–3090, (2016).

[7]. H. Zhao, D.R. White, T. Debroy, "*Current issues and problems in laser welding of automotive aluminium alloys*", International Materials Reviews, Vol. 44, No. 6, pp. 238-266, (2013).
[8]. Muralimohan Cheepu, *et al.*, "*Optimization of process parameters using surface response methodology for laser welding of titanium alloy*", Materials science forum, Vol. 969, pp. 539-545, (2019).
[9]. Mengxin Sun, Zhenwei Cao, Lukai Zheng, *"Design and Experiment of a Clamping-Drive Alternating Operation Piezoelectric Actuator",* MDPI, Micromachines, *Vol. 14, No. 3,* (2023).

TÓM TẮT

Nghiên cứu thiết kế hệ thống tạo biên dạng 2D áp dụng trong công nghệ hàn laser sử dụng bộ truyền động áp điện tuyến tính

Ngày nay, công nghệ laser được nghiên cứu và áp dụng trong nhiều lĩnh vực, trong đó có kỹ thuật hàn. Bài báo trình bày nghiên cứu thiết kế hệ thống tạo ra biên dạng 2D sử dụng trong công nghệ hàn laser. Hệ thống có thể tạo ra biên dạng bất kỳ, phù hợp với đặc tính và vật liệu của phôi hàn, từ đó, làm tăng chất lượng, độ chính xác, tính thẩm mỹ của mối hàn, cũng như nâng cao hiệu suất hàn laser. Trong bài báo, nhóm tác giả đề xuất mô hình hệ thống tạo ra biên dạng 2D sử dụng một gương phản xạ và hai bộ truyền động tuyến tính áp điện. Các phương trình động học thuận và nghịch được nhóm tác giả đưa ra và giải quyết triệt để, đồng thời nhóm cũng trình bày thuật toán để điều khiển chuyển động của các bộ truyền động tuyến tính. Mô hình được mô phỏng trên Matlab với biên dạng hình tròn, hình sin và hình số 8. Kết quả thu được cho thấy biên dạng thu được gần như giống với biên dạng mong muốn (cả hình dạng và chu kỳ quét). Có sự dịch chuyển giữa các biên dạng. Với các thông số mô phỏng đã cho, độ dịch chuyển của các biên dạng nói trên lần lượt là 0,03 mm (1,5%), 0,05 mm (2,5%) và 0,05 mm (1,25%). Sự dịch chuyển này có thể được giảm xuống bằng cách tăng số lần lấy mẫu. Các kết quả mô phỏng cung cấp bằng chứng mạnh mẽ về tính khả thi của việc triển khai hệ thống tạo biên dạng laser 2D thực tế dựa trên mô hình đề xuất.

Từ khoá: Biên dạng laser; Hàn laser; Hàn không tiếp xúc; Bộ truyền động áp điện tuyến tính.